Geomechanics and Engineering, *Vol. 6, No. 5 (2014) 469-485*
DOI: http://dx.doi.org/10.12989/gae.2014.6.5.469

Decrease trends of ultimate loads of eccentrically loaded model strip footings close to a slope

Evrim Cure [a], Erol Sadoglu [b], Emel Turker [c] and Bayram Ali Uzuner [*]

Department of Civil Engineering, Karadeniz Technical University, 61080 Trabzon, Turkey

(*Received June 03, 2013, Revised November 30, 2013, Accepted December 13, 2013*)

Abstract. A series of bearing capacity tests was conducted with eccentrically loaded model surface and shallow strip footings resting close to a slope to investigate behavior of such footings (ultimate loads, failure surfaces, load-displacement curves, rotation of footing, etc.). Ultimate loads of footing close to slope decreased with increasing eccentricity for both surface and shallow footings. Failure surfaces were not symmetrical, primary failure surfaces occurred on the eccentricity side (the slope side) and secondary failure surfaces occurred on the other side. Lengths of failure surfaces decreased with increasing eccentricity. Footings always rotated towards eccentricity side a few degrees. For eccentrically loaded footing, decrease in ultimate load with increasing eccentricity is roughly in agreement with Customary Analysis.

Keywords: bearing capacity; eccentrically loaded footings; footings resting close to slope; strip footings; plane-strain conditions

1. Introduction

Sometimes footings of structures may sit close to a slope (Fig. 1).

Eccentricity (e) is defined as M/Q, where M is moment, Q is vertical load for a footing (Fig. 2). Moment generally comes from lateral forces (earthquakes, lateral earth pressures, water, wind, brake forces, etc.) acting on structures. Today, almost all footings are subjected to moments due to lateral forces acting on structures. In Turkey, the Turkish Earthquake Code (2007) gives some eccentricity to the pure centrally loaded footings and all footings are designed as eccentrically loaded. Currently there is no available method to design eccentrically loaded strip footing sitting close to a slope. In other words, it is not known how much reduction should be done in ultimate load of centrally loaded footing close to a slope due to eccentricity to find the ultimate load of eccentrically loaded footing close to a slope.

It is known that an eccentrically loaded footing resting on continuous flat soil carries less load than the same centrally loaded footing resting on continuous flat soil ($Q_{ue} < Q_{uc}$ where Q_{ue} is the ultimate load of eccentrically loaded footing resting on continuous flat soil and Q_{uc} is the ultimate load of centrally loaded footing resting on continuous flat soil.). (Fig. 3) and that the ultimate load

*Corresponding author, Professor, Dr., E-mail: uzuner@ktu.edu.tr
[a] Research Assistant, Dr., E-mail: evrimcure@ktu.edu.tr
[b] Assistant Professor, Dr., E-mail: esadoglu@ktu.edu.tr
[c] Research Assistant, Dr., E-mail: emelturker@ktu.edu.tr

http://www.techno-press.org/?journal=gae&subpage=7 ISSN: 2005-307X (Print), 2092-6219 (Online)

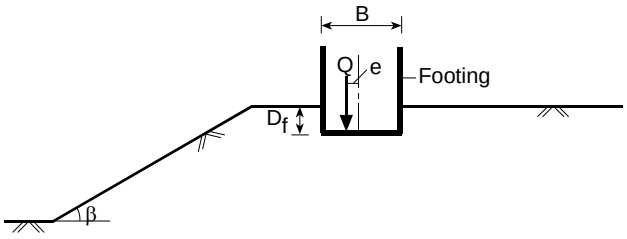

Fig. 1 An eccentrically loaded strip footing

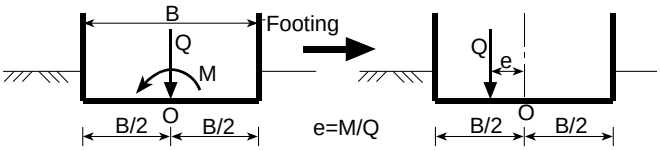

Fig. 2 Definition of eccentricity in a strip footing

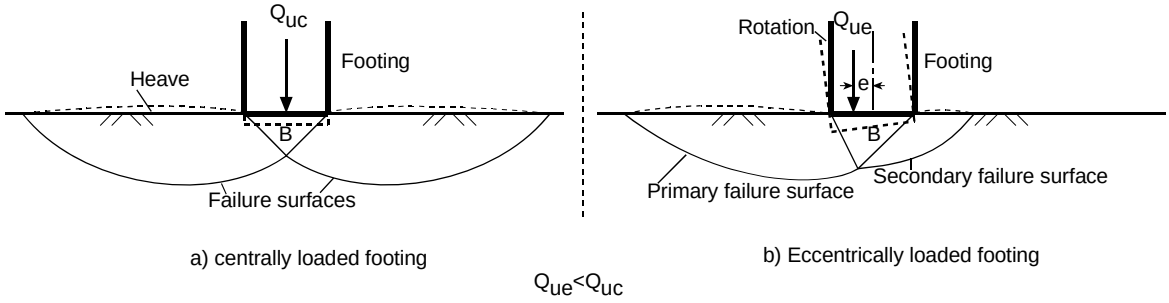

Fig. 3 Behaviors of the centrally and eccentrically loaded strip footings resting on continuous flat soil

of the eccentrically (Q_{ue}) loaded footing decreases with increasing eccentricity.

This decrease can be explained as follows: Roughly, the ultimate load of a footing can be considered as an effort to shear the soil mass along failure surfaces. Failure surfaces of a centrally loaded footing on horizontal flat soil are symmetrical (Fig. 3(a)). On the other hand, failure surfaces of an eccentrically loaded footing resting on continuous flat soil are not symmetrical (Fig. 3(b)), since the footing rotates towards the eccentricity side, a primary failure surface develops on the eccentricity side and a secondary failure surface occurs on the other side (Moroglu *et al*. 2005, Sadoglu *et al*. 2009). Thus, total area (or length) of eccentrically loaded footing's failure surfaces is less than the same centrally loaded footing's, so ultimate loads are different accordingly. There are mainly two methods to calculate this decrease: Meyerhof's Effective Width Concept and Customary Analysis (Traditional Method, Conventional Theory).

Meyerhof (1953) put forward that the ultimate load (Q_{ue}) of an eccentrically loaded strip foundation having a width B is equal to the ultimate load (Q_{uc}') of the centrally loaded strip foundation having a reduced width B' obtained by subtracting 2e from B.

Some assumptions are made in Customary Analysis in order to determine the normal base pressure distributions under an eccentrically loaded footing. These are: Stress distribution is linear, there are equilibrium for vertical forces ($\Sigma V = 0$) and moments ($\Sigma M = 0$) and the contact is lost between the footing base and the soil where tensile stresses occur. Uzuner (1975) investigated the base stress distribution of eccentrically loaded model strip footings on continuous flat sand experimentally and concluded that the assumptions of Customary Analysis are satisfactory. The base stress distributions of a strip footing are shown in Fig. 4. The ultimate load of eccentrically loaded strip footing can be determined from the following condition according to the Customary Analysis: The value of the maximum base pressure (q_{max}) should not exceed the ultimate bearing capacity (q_u) of the same centrally loaded strip footing ($q_{max} \leq q_u$) (Duncan *et al*. 1990). According to Customary Analysis an eccentrically loaded strip footing carries smaller loads, by as much as the inclined hatched areas in Fig. 4**,** than the same centrally loaded one.

The ratio Q_{ue}/Q_{uc} becomes as following in the Customary Analysis

$$\frac{Q_{ue}}{Q_{uc}} = \frac{1}{1+\frac{6e}{B}} \quad \text{(inside and on the core (kern, middle - third), } e \leq B/6) \tag{1}$$

$$\frac{Q_{ue}}{Q_{uc}} = \frac{3}{4}\left(1-\frac{2e}{B}\right) \quad \text{(outside the core, } e > B/6) \tag{2}$$

If 1/12, 1/6 and 1/3 are put in place of *e/B* in Eqs. (1) and (2), the Q_{ue}/Q_{uc} ratio becomes, 0.67, 0.5 and 0.25 respectively. These ratios are independent of the shape of the footing, depth of footing, slope angle, etc. (Moroglu *et al*. 2005, Sadoglu *et al*. 2009). Customary Analysis is an anonymous method, so a certain reference cannot be given. This method is used mostly to determine base stress distributions of rigid footings and reduction in ultimate load of eccentrically loaded footing due to eccentricity.

A centrally loaded footing resting close to a slope carries smaller load than the same footing on horizontal flat soil, because the length of one of the failure surfaces is short due to the existence of the slope. There are experimental and theoretical works for such footings (Fig. 5).

Centrally and eccentrically loaded footings on continuous flat soils were investigated by many researchers (Youssef Abdel Massih *et al*. 2008, Vessia *et al*. 2009, Shahin and Cheung 2011, Ornek *et al*. 2012, etc.).

Centrally loaded strip footings sitting close to slopes were studied experimentally by several researchers (Lebegue 1973, Shields *et al*. 1977, Bauer *et al*. 1981, Kusakabe *et al*. 1981, Clark

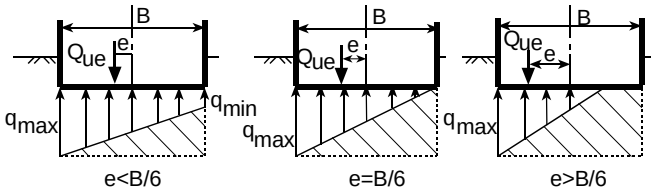

Fig. 4 The base normal stress distributions in Customary Analysis

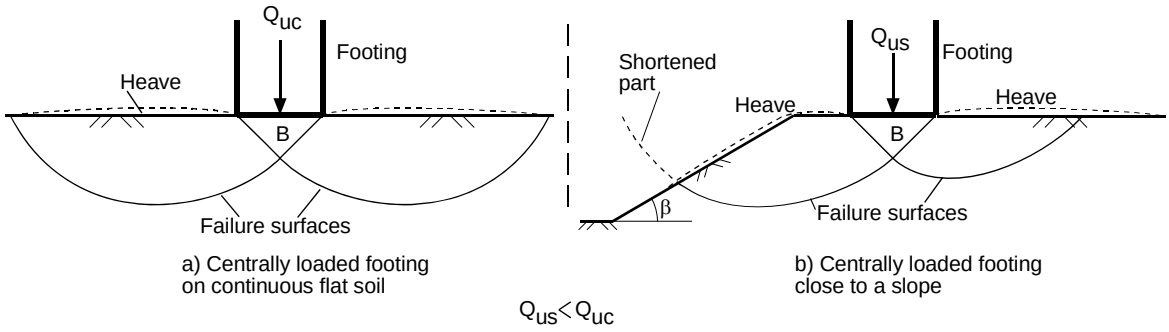

Fig. 5 Behaviors of the same footing on continuous flat soil and close to a slope

et al. 1988, Gemperline 1988, Georgiadis *et al*. 2013, etc.). There are some theoretical studies for calculating ultimate loads of centrally loaded strip footings sitting close to slopes (Meyerhof 1957, Mizuno *et al*. 1960, Hansen 1970, Chen 1969, Vesic 1973, 1975, Graham *et al*. 1988, Saran *et al*. 1989, Shields *et al*. 1990, Bowles 1996, etc.).

Eccentrically loaded strip footings resting close to slope has attracted little attention from researchers. Saran and Reddy (1990) developed an approach to calculate bearing capacity factors from ultimate loads of eccentrically loaded footings resting close to slopes. Unfortunately they didn't carry out tests for comparison.

In this work, ultimate loads of an eccentrically loaded surface and shallow strip footing resting close to a slope and other matters such as decrease of ultimate load with increasing eccentricity, failure surfaces, load-displacement curves, rotations, etc. of footings were examined experimentally. This work is a continuation of works of Moroglu *et al*. (2005) and Sadoglu *et al*. (2009).

2. Experimental work

The experimental system was used for footings sitting close to a slope for this work. The primary components of the experimental set up are a tank, model strip footing, loading system, sand, etc.. These are explained below. More details of the experimental system can be found elsewhere (Moroglu 2002, Moroglu *et al*. 2005, Sadoglu 2009, Sadoglu *et al*. 2009).

2.1 The tank

The internal dimensions of the tank containing the sand are 0.9 m (length, L) × 0.10 m (width, W) × 0.65 m (height, H) (Figs. 6 and 7). The bottom and the sides of the tank were produced using hard wood. The front and back sides of the tank were constructed of 20 mm thick glass plates to observe failure surfaces.

The strip footing case corresponds to a plane strain condition. There are mainly two conditions for the plane strain case. Firstly, deformation in W direction should be 'zero' ($\varepsilon_y = 0$, where $\varepsilon_y = \Delta W/W$, ε_y is strain in W direction, ΔW is total lateral displacement of tank's sides, W is tank width)

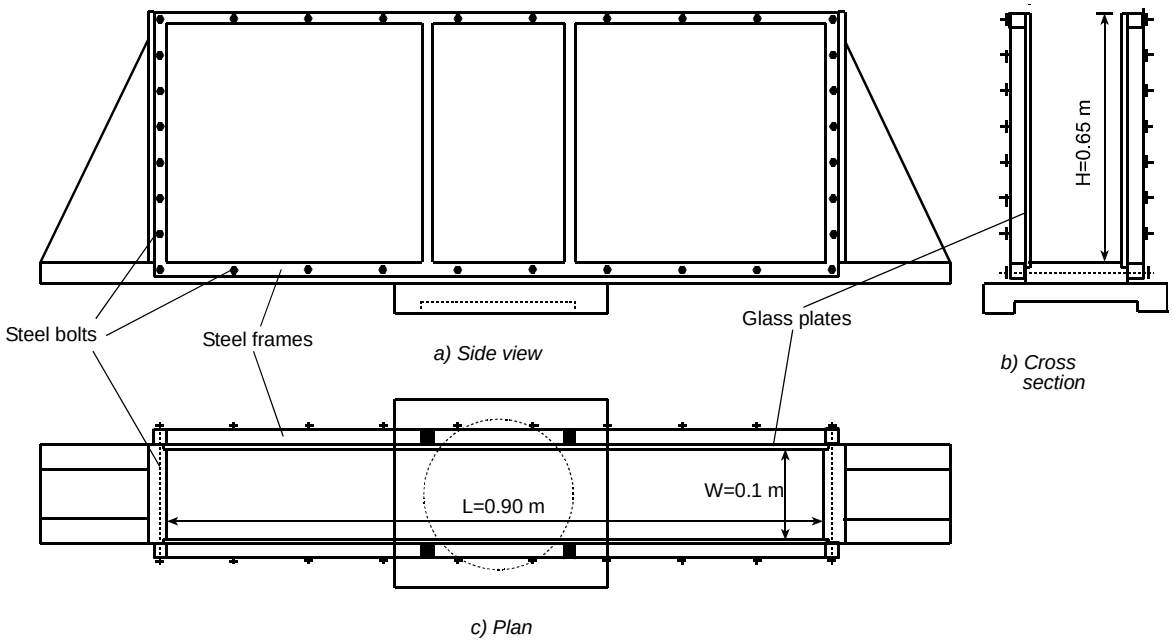

Fig. 6 Three views of the tank

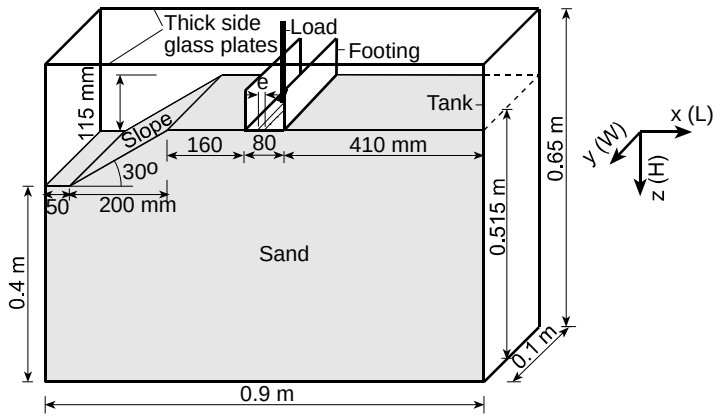

Fig. 7 Three dimensional schematic view of the experimental system

(Fig. 7). This implies that plane strain models should have 'rigid' front and back sides. Secondly, friction between soil and the front and back internal surfaces of the tank should be 'zero'. This implies full frictionless internal surfaces. Since these conditions cannot be met absolutely in models, some criteria should be fulfilled. Otherwise experimental results may contain serious errors and may not represent a plane strain case (Ko and Davidson 1973, Kirkpatrick and Yanikian 1975, etc.).

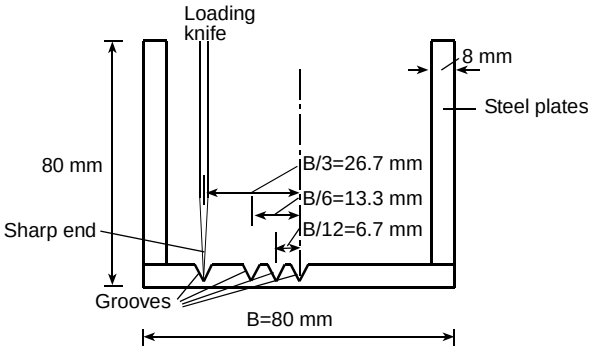

Fig. 8 The model strip footing

Kirkpatrick and Yanikian (1975) proposed that ε_y should be less than 0.1% for plane strain models. Two steel frames made of hollow sections were produced and connected to each other with steel bolts along the edges of the frames. Steel elements made of solid profiles were welded in the middle part of the frames to prevent deformation of the glass plates. The surface of the steel frame on which glass plates touch was produced to be almost perfect plane so that no glass plate was broken during tests. Two dial gauges were placed on the external faces of the glass plates to measure lateral deformations. Measured horizontal displacements and calculated strains of the sides were found to be well less than 0.1% in the tests.

Ideally, thin latex sheets should be placed on the internal faces of the lightly lubricated glass plates to achieve almost frictionless side faces. This application has difficulties due to movements of the sand mass in different directions. The sand is in contact with glass faces directly in this experimental work. Kirkpatrick and Uzuner (1975) showed that the effect of side friction between glass sides and sand on bearing capacity is less than 10% in case of $B/W = 1$ (B: footing width, W: tank width) for a surface footing sitting on medium dense sand. The conditions of this experimental work are close to the conditions of the work done by Kirkpatrick and Uzuner (1975). Moreover, the effect of side friction is approximately eliminated in this experimental work due to usage of the ratios of the ultimate loads instead of the ultimate loads.

2.2 The model footing

The model strip footing was produced by welding 8 mm thick steel plates together for rigid footing conditions (Fig. 8). The dimensions of the footing in the test set up are 80 mm (width, B) × 100 mm (length) × 80 mm (height). V shaped grooves were opened along the length of the base plate so different eccentricities (inside, on the boundary and outside of the core, e = 0, 6.7, 13.3, 26.7 mm or e/B = 0, 1/12, 1/6, 1/3) could be applied. A thickness of 2 mm was left under the grooves, so eccentricity did not change substantially during tests of the rotating footing. The footing base was covered by coarse sandpaper to obtain a full frictional condition along the base of the footing.

2.3 The sand

The sand used in tests was local Black Sea Coastal Sand and it has a grain size distribution that

ranges from about 0.2 to 4 mm (medium-coarse) and is classified as *SP* (poorly graded). Properties of the sand are summarized in Table 1. The internal friction angles of the sand were measured from shear box (60 mm × 60 mm) and triaxial (D = 38 mm) tests at the relative density, D_r, of 0.74. Vertical stresses of 25, 50, 100 kPa in shear box test and confining pressures of 25, 50, 100 kPa in triaxial test were applied. In literature, it is reported that there is a relation between ϕ_{sb}, ϕ_{tr} and ϕ_{ps} (ϕ_{sb}: shear box, ϕ_{tr}: triaxial, ϕ_{ps}: plane strain) (Cornforth 1964).

$$\phi_{sb} < \phi_{tr} < \phi_{ps} \tag{3}$$

The difference between these internal friction angles could be up to 8°.

Shear box (ϕ_{sb}) and triaxial (ϕ_{tr}) values of internal friction angles of the sand at D_r = 0.74 were determined as 41° (ϕ_{sb}) and 43° (ϕ_{tr}), respectively (Table 1). Ideally the plane strain internal friction angle (ϕ_{ps}) should be used for strip footings. Because of the fact that we do not have experimental facilities to determine ϕ_{ps} of the sand, the plane strain internal friction angle of sand (ϕ_{ps}) was taken as 48° using the formula proposed by Lade and Lee (1976).

$$\phi_{ps} = 1.5\phi_{tr} - 17^{\circ} (\phi_{tr} > 34^{\circ}) \tag{4}$$

The sand was placed in the tank at sufficient density so that general shear failure can be obtained in the tests and the relative density (D_r) was kept constant throughout all the tests as 0.74 (ρ_{dry} = 1.581 Mg/m^3). The sand was placed in 50 mm thick layers to achieve 400 mm flat height and 115 mm slope height in the tank (Fig. 9). For surface strip footing tests, the quantity (7112 g) for a 50 mm thick layer was deposited in the tank loosely as a uniform thick (about 57 mm) layer. This loose sand layer was lightly compacted with a wooden hammer in the tank to about 50 mm thick layer. To confirm 50 mm thickness, horizontal lines at 50 mm intervals were drawn on the internal face of the glass plate. This process continued until the sand mass height reached 0.40 m (5B). Then, for a 115 mm slope height, 3 wooden wedges were used (Fig. 7). The reason of forming the slope in three layers was to obtain smooth slope surface. The first wooden wedge was placed on the 400 mm flat soil mass and the quantity (6382 g) for a 50 mm thick layer was

Table 1 Properties of the sand used in the tests

Property	Quantity
Specific gravity, G_s	2.66
Maximum dry density, $\rho_{dry(max)}$ (Mg/m^3)	1.658
Minimum dry density, $\rho_{dry(min)}$ (Mg/m^3)	1.395
Effective size, D_{10} (mm)	0.58
D_{30} (mm)	0.80
D_{60} (mm)	0.95
Coefficient of uniformity, C_u	1.64
Coefficient of curvature, C_r	1.16
Angle of internal friction, $\phi_{\text{direct shear}}$ (degrees)	41
Angle of internal friction , ϕ_{triaxial} (degrees)	43

deposited in the tank. The second wooden wedge was placed on first wooden wedge and the quantity (5704 g) for a 50 mm thick layer was deposited in the tank. Lastly, the same process was repeated for a 15 mm thick layer. After the sand deposit process was finished, 80 mm width model footing was placed on flattened surface of the sand. For a shallow strip footing, test steps explained above are the same, but after placing 80 mm width model footing, a 20 mm thick surcharge (D_f/B = 0.25, D_f: depth of footing) was formed at the sides of the footing. A 0.515 m depth of sand under the footing was thought to be sufficient, since significant depth (the most influenced depth) is taken as (3-4)B for strip foundations in practice. The dry density of deposited sand (or relative density) in the tank was calculated by weighing the sand mass removed from the tank. Before actual tests, several sand depositions in the tank were made. Good agreement was found in these trials. The error in relative density was calculated to be less than 1% in these trials.

2.4 The loading system

The loading frame from a triaxial apparatus was used for the application of the vertical load. The general scheme of the loading system is seen in Fig. 9. The capacity of the loading frame is 10 kN and its vertical constant displacement rate was chosen as 0.15 mm/min. The tank sat on the head of the triaxial piston with a round socket under it. The loading was applied with a sharp edge of a loading knife resting on selected grooves according to the eccentricity by taking reaction

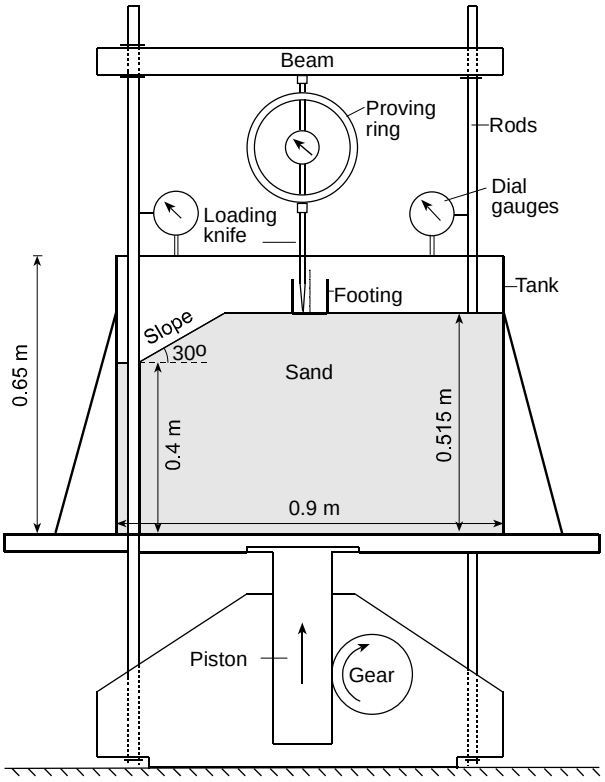

Fig. 9 The loading system for strip footing tests

through a proving ring from the upper beam of the press as seen in Fig. 9. The proving ring has a 6 kN capacity. The rise of the tank was measured by mounting two dial gauges to the side rods of the press. The vertical displacement of the footing was obtained by subtracting the deformation of the proving ring from the average rise of the tank.

2.5 Running of a typical test

The sand was deposited in the tank using a procedure described above. Before the 80 mm width model footing was placed at a distance of 160 mm ($D_e = 2B$) from the slope edge (Fig. 9), the surface of the sand was flattened by a special device travelling backwards and forwards and cutting the sand mass from top and accumulating sand at the side of the tank without disturbing the sand. The accumulated sand was removed with a special shovel. The upper beam was mounted and the loading mechanism with the footing was lowered on the sand. Two dial gauges were mounted to the press rods and the other two dial gauges were mounted on the glass walls. The loading was started and readings from all dial gauges were taken at regular time intervals. Failure (maximum load) was reached and after formation of failure surfaces, the test was stopped and the system was disassembled. The sand was emptied through 2 holes under the tank, weighed and its density was determined. In addition, during loading a digital camera was used to take photographs through the glass plate at regular time intervals. A stereo-photogrammetric technique (Butterfield *et al*. 1970) was used to find out failure surfaces by taking pictures from a constant camera. Thus, failure surfaces were drawn for each test.

3. Results and discussion

For a model surface (footing width, B = 80 mm, depth of the footing, D_f = 0 mm, so D_f/B = 0) and shallow footing (footing width, B = 80 mm, depth of the footing, D_f = 20 mm, so D_f/B = 0.25), a series of tests was performed with different eccentricities (e/B = 0 (centered), 1/12 (inside the core), 1/6 (on boundary of the core, 1/3 (outside the core)) on dense (D_r = 0.74) sand and each test was repeated twice (a and b). The results of total number of tests, 16, are given in Table 2. The difference in ultimate loads (Q_{us}) was less than 3% in repeated tests. Average ultimate loads ($Q_{us\,(av.)}$) for every case were calculated and can be seen in Table 2.

3.1 Failure surfaces

As an example, for Test 2a (Table 2) primary and secondary failure surfaces for an eccentrically of e/B = 1/12 loaded model surface strip footing resting close to the slope are given in Fig. 10. This failure mechanism is typical for other tests. It is seen that failure surfaces of eccentrically loaded footings sitting close to the slope were not symmetrical, primary failure surfaces occurred on the eccentricity side and secondary failure surfaces occurred on the other side.

Footings always rotated to the eccentricity side for this eccentrically loaded footing sitting close to the slope. The footing rotations were not measured but evaluated as a few degrees. The rotation angle increased with increasing eccentricity.

The failure surfaces for all eccentricity cases of surface footings are given in Fig. 11. It is seen that the horizontal distances (L_f) between the intersections of the failure surfaces with the slope and footing side decreased with increasing eccentricity. Similar results are valid for shallow footings.

Table 2 The results of the tests

Test No	e/B	D_f (mm)	D_f/B	Q_{us} (kN)	ΔH_f (mm)	$Q_{us\,(av.)}$ (kN)	$Q_{us\text{-}sur.}/Q_{us\text{-}sha.}$
1a-sur.	0	0	0	2.05	4.05	2.06	
1b-sur.	0	0	0	2.08	4.21		
2a-sur.	1/12	0	0	1.38	3.36	1.40	
2b-sur.	1/12	0	0	1.42	3.40		
3a-sur.	1/6	0	0	1.02	2.37	1.02	
3b-sur.	1/6	0	0	1.02	2.51		
4a-sur.	1/3	0	0	0.38	1.63	0.38	
4b-sur.	1/3	0	0	0.38	1.71		
1a-sha.	0	20	0.25	2.53	4.19	2.55	1.23
1b-sha.	0	20	0.25	2.56	4.50		
2a-sha.	1/12	20	0.25	1.76	3.43	1.76	1.26
2b-sha.	1/12	20	0.25	1.76	3.52		
3a-sha.	1/6	20	0.25	1.30	2.57	1.31	1.28
3b-sha.	1/6	20	0.25	1.32	2.47		
4a-sha.	1/3	20	0.25	0.53	2.07	0.54	1.43
4b-sha.	1/3	20	0.25	0.54	2.11		

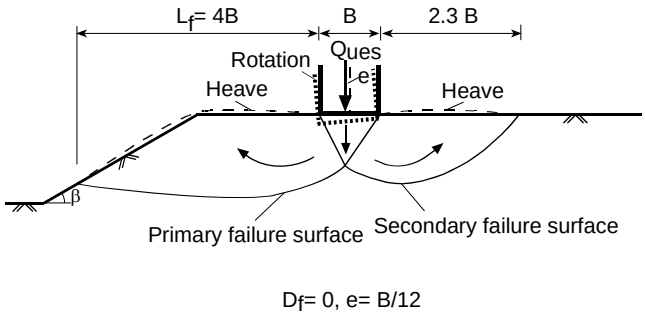

Fig. 10 Failure surfaces for eccentrically loaded model surface strip footing resting close to slope (Test 2a sur.)

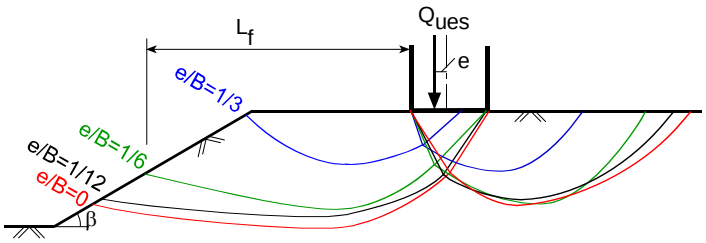

Fig. 11 Horizontal distances between the intersections of the failure surfaces with sand slope surface and footing side

These observations supported the findings that ultimate loads of eccentrically loaded footings sitting close to the slope decreases with increasing eccentricity, since the ultimate load is relevant to total area or length of failure surfaces.

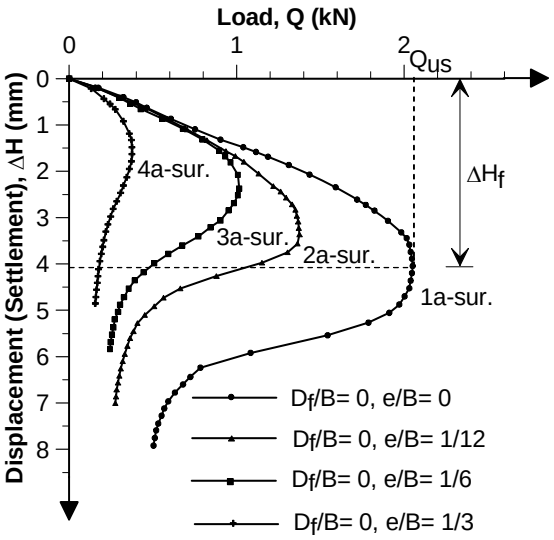

(a)

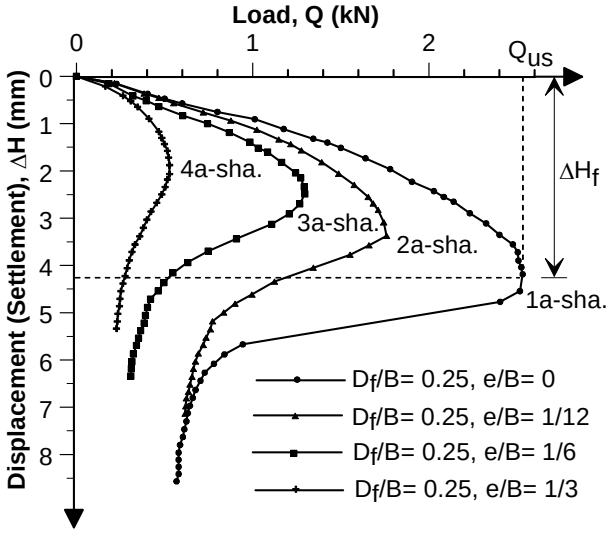

(b)

Fig. 12 The load-displacement relations for model surface (a) and shallow (b) strip footing resting close to slope

3.2 Load-displacement relations

In Figs. 12(a) and (b), experimental load-displacement relations are seen (Table 2). In all tests, general shear failures occurred as expected due to the dense sand condition and the load dropped after failure.

Vertical displacement values at failure (ΔH_f) decreased with increasing eccentricity. ΔH_f values are a little bigger in shallow footings than surface footings (Table 2).

3.3 Ultimate loads

For comparison, experimental ultimate loads of centrally loaded surface and shallow footings sitting close to the slope were compared with Bowles approach (Bowles 1996). Bowles approach was selected, because it is the most updated one. Comparison is seen in Table 3. From Table 3, it can be seen that experimental results are in agreement with Bowles results. The difference in ultimate loads between experimental and Bowles results are within 10%.

Table 3 Comparison of centrally loaded model surface and shallow strip footing (B= 0.08 m) test results with Bowles Approach

Conditions	$Q_{us\,(av.)}$ (Experimental) (kN)	Q_{us} (Bowles) (kN)
e = 0, D_f/B = 0	2.06	1.86
e = 0, D_f/B = 0.25	2.55	2.42

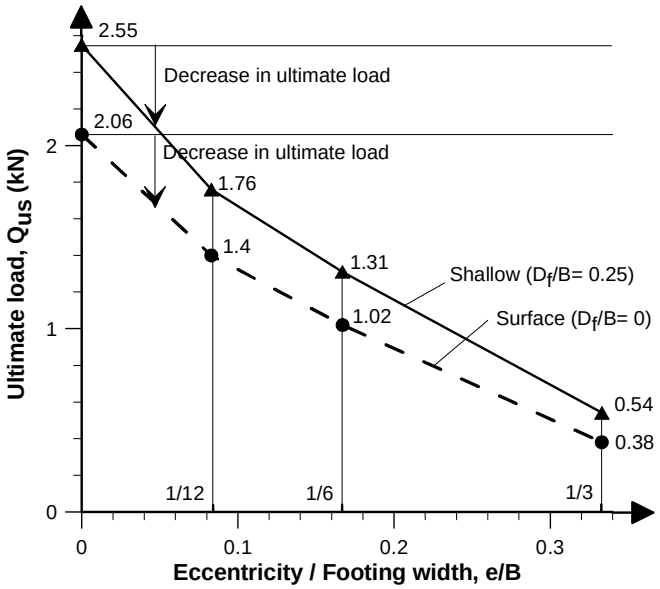

Fig. 13 The experimental relations between Q_{us} and e/B for the model surface and shallow strip footing resting close to slope

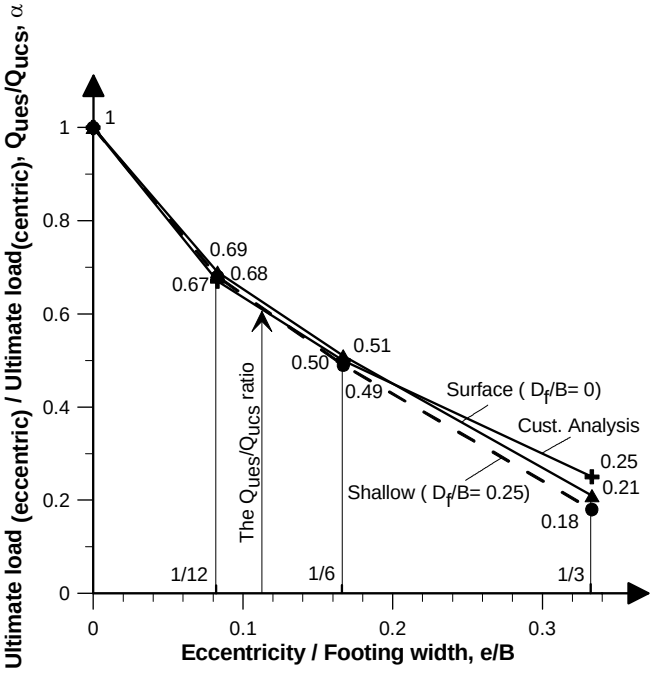

Fig. 14 The experimental relations between Q_{ues}/Q_{ucs} ratio and e/B for the model surface and shallow strip footing resting close to slope

Experimental relations between ultimate loads and eccentricities for current footings sitting close to the slope are seen in Fig. 13. Average ultimate loads were used in Figs. 13 and 14. The ultimate loads decreased with increasing eccentricities in both the surface and shallow cases. As expected the decrease in ultimate loads with increasing eccentricities in tests with the shallow footings are bigger than for the surface footings.

Experimental ultimate load ratios-eccentricity/footing width ratios relation (Q_{ues}/Q_{ucs}-e/B) is given in Fig. 14. The Q_{ues}/Q_{ucs} ratio can be expressed as a dimensionless factor and this factor (a reduction factor, α) is less than 1. If this factor is known, the ultimate load of an eccentrically loaded footing resting close to a slope can be estimated by multiplying the ultimate load of a centrally loaded footing with this factor ($Q_{ues} = Q_{uec}$). In Fig. 14, the Q_{ues}/Q_{ucs} ratios for $D_f/B = 0$ are slightly larger than the $D_f/B = 0.25$ case.

Experimental relations in Figs. 13 and 14 could not be compared with the Saran and Reddy approach, since Saran and Reddy prepared graphs of the bearing capacity coefficients up to 40° of internal friction angle.

Although the Customary analysis is for eccentrically loaded footings resting on horizontal flat soil surface, it was thought that it would be interesting to compare experimental results with Customary analysis. Fig. 14 shows a comparison of experimental results with Customary analysis. Experimental ratios are close to Customary analysis.

This experimental work is performed at small scale. Since ratios of ultimate loads and mostly surface footings are used, scale effect is eliminated.

4. Conclusions

Bearing capacity tests on an eccentrically loaded model strip footings resting close to a slope were performed with an experimental set up in plane strain conditions (especially deformation condition). From the experimental test results, the following conclusions can be deduced:

- General shear failures occurred in dense sand conditions. Primary failure surfaces occurred on the eccentricity side, secondary on the other side and length of failure surfaces decreased and staged closer to the surface with increasing eccentricity. The footing rotated towards the eccentricity side a few degrees. Vertical displacement movement values to reach failure decreased with increasing eccentricity. Horizontal distance between the intersections of the failure surfaces with sand slope surface and footing side decreased with increasing eccentricity.
- Experimental ultimate loads of eccentrically loaded strip footings sitting close to slope decreased with increasing eccentricity. This decrease is due to eccentricity and slope. Decrease in ultimate loads follows roughly Customary analysis. Until refined approaches are introduced, these experimental decrease ratios can be used for dense condition or Customary analysis can be applied roughly to design such footings. Obviously, more research is needed in this area.
- Ultimate loads of centrally loaded surface and shallow footing sitting close to slope are in agreement with Bowles's approach.

In this experimental work, behavior (ultimate loads, failure surfaces, rotation of footing, etc.) of eccentrically loaded footing sitting close to slope was investigated and some lights were thrown on such footings.

References

Bauer, G.E., Shields, D.H., Scott, J.D. nd Gruspier, J.E. (1981), "Bearing capacity of footings in granular slopes", *Proceedings of the Tenth International Conference on Soil Mechanics and Foundation Engineering*, Balkema, Rotterdam, The Netherlands, Vol. 2, pp. 33-36.

Bowles, J.E. (1996), *Foundation Analysis and Design*, McGraw-Hill International Editions, (Fifth Edition), New York, 1175.

Butterfield, R., Harkness, R.H. and Andrawes, K.Z. (1970), "A stereo-photogrammetric method for measuring displacement fields", *Geotechnique*, **20**(3), 308-314.

Chen, W.F. (1969), *Limit Analysis and Soil Plasticity*, Elsevier Scientific Publishing Company.

Clark, J.I., McKeown, S. and Crawford, C.B. (1988), "Field measurements of the behaviour of inclined footings on a natural slope", *Can. Geotech. J.*, **25**(4), 662-674.

Cornforth, D.H. (1964), "Some experiments on the influence of strain conditions on strength of sand", *Geotechnique*, **14**(2), 143-167.

Duncan, J.M., Clough, C.W. and Ebeling, R.M. (1990), "Design and performance of earth retaining structures", *Geotech. Special Publication*, *ASCE*, **25**, 251-277.

Gemperline, M.C. (1988), "Centrifuge modeling of shallow foundations", *Proceedings of ASCE Spring Convention*, *ASCE*, pp. 45-70.

Georgiadis, K., Georgiadis, M. and Anagnostopoulos, C. (2013), "Lateral bearing capacity of rigid piles near clay slopes", S*oil. Found.*, **53**(1), 144-154.

Graham, J., Andrews, M. and Shields, D.H. (1988), "Stress characteristics for shallow footings in cohesionless slopes", *Can. Geotech. J.*, **25**(2), 238-249.

Hansen, J.B. (1961), "A general formula for bearing capacity", *Danish Geotech. Inst.*, Copenhagen, Bulletin

No. 11, 46.
Hansen, J.B. (1970), "A revised and extend formula for bearing capacity", *Danish Geotech. Inst.*, Copenhagen, Bul. No. 28, 21 (successor to Bul. No. 11).
Kirkpatrick, W.M. and Uzuner, B.A. (1975), "Measurement errors in model foundations tests", *Istanbul Conference on Soil Mechanics and Foundation Engineering*, Istanbul, Turkey, March-April, pp. 98-106.
Kirkpatrick, W.M. and Yanikian, H.A. (1975), "Side friction in plane strain tests", *Proceedings of the fourth Southeast Asian Conference on Soil Engineering*, Kuala Lumpur, Malaysia, April, pp. 76-84.
Ko, H. and Davidson, W. (1973), "Bearing capacity of footings in plane strain", *J. SM & FE Div.*, *ASCE*, **99**(1), 1-23.
Kusakabe, O., Kimura, T. and Yamaguchi, H. (1981), "Bearing capacity of slopes under strip loads on the top surfaces", *Soil. Found.*, 21(4), 29-40.
Lebegue, Y. (1973), "Essais de foundations superficielles sur talus", *Proceedings of the 8th International Conference on Soil Mechanics and Foundation Engineering*, Moscow, Russia, 4(3), pp. 313.
Lade, P.V. and Lee, K.L. (1976), "Engineering properties of soils", *Engineering Report*, UCLA-ENG-7652, Los Angeles, CA, USA, pp. 145.
Meyerhof, G.G. (1953), "The bearing capacity of foundations under eccentric and inclined loads", *Proceedings of the 3rd International Conference on Soil Mechanics and Foundation Engineering*, Switzerland, August, Session 1, pp. 440-445.
Meyerhof, G.G. (1957), "The ultimate bearing capacity of foundations on slopes", *Proceedings of the Fourth International Conference on Soil Mechanics and Foundation Engineering*, London, UK, August, Vol. 1, pp. 384-386.
Mizuno, T., Takumitsu, Y. and Kawakami, H. (1960), "On the bearing capacity of a slope of cohesionless soil", *Soil. Found.*, **1**(2), 30-37.
Moroglu, B. (2002), "The bearing capacity of the eccentrically loaded model strip footing on reinforced sand", Ph.D. Thesis, Karadeniz Technical University, Trabzon, Turkey. [In Turkish]
Moroglu, B., Uzuner, B.A. and Sadoglu, E. (2005), "Behaviour of the model surface strip footing on reinforced sand", *Indian J. Eng. Mater. Sci.*, **12**(5), 419-426.
Ornek, M., Laman, M., Demir, A. and Yildiz, A. (2012), "Prediction of bearing capacity of circular footings on soft clay stabilized with granular soil", *Soil. Found.*, **52**(1), 69-80.
Sadoglu, E. (2009), "The bearing capacity of the eccentrically loaded model shallow strip footing on reinforced sand", Ph.D. Thesis, Karadeniz Technical University, Trabzon, Turkey. [In Turkish]
Sadoglu, E., Cure, E., Moroglu, B. and Uzuner, B.A. (2009), "Ultimate loads for eccentrically loaded model shallow strip footings on geotextile-reinfoced sand", *Geotext. Geomembr.*, **27**(3), 176-182.
Saran, S. and Reddy, B.S. (1990), "Bearing capacity of eccentrically loaded footings adjacent to cohesionless slopes", *Indian Geotech. J.*, **20**(2), 119-142.
Saran, S., Sud, V.K. and Handa, S.C. (1989), "Bearing capacity of footings adjacent to slopes", *J. Geotech. Eng.*, *ASCE*, **115**(4), 553-573.
Shahin, M.A. and Cheung, E.M. (2011), "Stochastic design charts for bearing capacity of strip footings", *Geomech. Eng., Int. J.*, **3**(2), 153-167.
Shields, D.H., Chandler, N. and Garnier, J. (1990), "Bearing capacity of foundations in slopes", *J. Geotech. Eng.*, **116**(3), 528-537.
Shields, D.H., Scott, J.D., Bauer, G.E., Deschenes, J.H. and Barsvary, A.K. (1977), "Bearing capacity of foundations near slopes", *Proceedings of the Ninth International Conference on Soil Mechanics and Foundation Engineering*, Tokyo, Japan, Vol. 1, pp. 715-720.
Turkish Earthquake Code (2007), "Specification structures to be built in disaster areas", Ministry of Public Works and Settlement, Government of Republic of Turkey, Turkey.
Uzuner, B.A. (1975), "Centrally and eccentrically loaded strip foundations on sand", Ph.D. Thesis, Strathclyde University, Glasgow, Scotland.
Vesic, A.S. (1973), "Analysis of ultimate loads of shallow foundations", *JSMFD, ASCE*, **99**(1), 45-73.
Vesic, A.S. (1975), *Bearing Capacity of Shallow Foundations*, Foundation Engineering Handbook, Winterkorn and Fang, (First Edition), New York, Van Nostrand Reinhold, 751.

Vessia, G., Cherubini, C., Pieczynska, J. and Pula, W. (2009), "Application of random finite element method to bearing capacity design of strip footing", *J. Geo Eng.*, **4**(3), 103-112.
Youssef Abdel Massih, D.S., Soubra, A. and Low, B.K. (2008), "Reliability-based analysis and design of strip footings against bearing capacity failure", *J. Geotech. Geoenviron. Eng.*, **134**(7), 917-928.

PL

Notation

B	footing width
B'	reduced width of footings
C_r	coefficient of curvature
C_u	coefficient of uniformity
Cust.	Customary
D	diameter
D_{10}	effective size
D_{30}	diameter at which 30% percentage passing
D_{60}	diameter at which 60% percentage passing
D_e	distance of the edge of the footing from the crest of the slope
D_f	depth of footing
D_r	relative density
e	eccentricity
G_s	specific gravity
H	tank height
L	tank length
L_f	horizontal distance between the intersections of the failure surfaces with sand slope surface and footing side
M	moment
Q	vertical load
$q_{\max}$	maximum value of base pressure distribution
Q_u	ultimate load
$Q_{u(av.)}$	average ultimate load
q_u	ultimate bearing capacity
Q_{uc}	ultimate load of centrally loaded footing resting on continuous flat soil
Q_{ue}	ultimate load of eccentrically loaded footing resting on continuous flat soil
Q_{us}	ultimate load of footing resting close to a slope

Q_{usc}	ultimate load of centrally loaded footing resting close to a slope
Q_{use}	ultimate load of eccentrically loaded footing resting close to slope
s	slope
sha.	shallow
SP	poorly graded sand
sur.	surface
u	ultimate
W	tank width
α	a reduction factor
β	slope angle
ΔH_f	vertical displacement value at failure
ΔW	total lateral displacement of tank's sides
ε_y	strain in longitudinal direction
ρ_{dry}	dry density
ΣM	algebraic sum of moments
ΣV	algebraic sum of vertical forces
$\rho_{\text{dry(max)}}$	maximum dry density
$\rho_{\text{dry(min)}}$	minimum dry density
ϕ_{ps}	plane strain internal friction angle
ϕ_{sb}	shear box internal friction angle
ϕ_{tr}	triaxial internal friction angle